European Journal of Medical Genetics 72 (2024) 104975

Contents lists available at ScienceDirect

European Journal of Medical Genetics

journal homepage: www.elsevier.com/locate/ejmg

A novel germline Pregnane X Receptor (*PXR*) variant predisposing to Hodgkin lymphoma in two siblings

Khusan Khodzhaev [a,b,1], Tugce Sudutan [a,b,1], Yucel Erbilgin [a], Merve Saritas [a,c], Gulcin Yegen [d], Ceyhun Bozkurt [e], Muge Sayitoglu [a,**,2], Rejin Kebudi [f,*,2]

[a] Genetics Department, Aziz Sancar Institute of Experimental Medicine, Istanbul University, Istanbul, Türkiye
[b] Institute of Health Science, Istanbul University, Istanbul, Türkiye
[c] Faculty of Life and Natural Sciences, Molecular Biology and Genetics Department, Abdullah Gul University, Kayseri, Türkiye
[d] Department of Pathology, Istanbul Medical Faculty, Istanbul University, Istanbul, Türkiye
[e] Department of Pediatric Hematology and Oncology, Istinye University, School of Medicine, Istanbul, Türkiye
[f] Oncology Institute, Division of Pediatric Hematology-Oncology, Istanbul University, Istanbul, Türkiye

ARTICLE INFO

Handling Editor: A. Verloes

Keywords:
Lymphoma
PXR
Germline predisposition
HRS cell
NF-κB

ABSTRACT

Hodgkin's lymphoma (HL) is the most common cancer in adolescents and young adults. A family history of HL increases the risk of developing HL in other family members. Identification of genetic predisposition variants in HL is important for understanding disease aetiology, prognosis, and response to treatment. Aberrant activation of the NF-κB pathway is a hallmark feature of HL, contributing to the survival and proliferation of the malignant cells' characteristic of HL.

The family with multiple consanguineous marriages with siblings of diagnosed HL was examined by whole-exome sequencing. We found a germline homozygous variation in the PXR ligand binding domain (NM_003889.3:c.811G>A, p.(Asp271Asn)), which was classified as pathogenic by prediction tools and segregated in HL cases. Increased *PXR* expression was found in homozygous variant carriers compared to heterozygous carriers by quantitative real time PCR (qRT-PCR) and immunofluorescence staining of patients' formalin-fixed paraffin-embedded tissues showed upregulation of PXR, particularly in Hodgkin Reed/Sternberg (HRS) cells.

Patients with homozygous *PXR* variant showed significantly high expression compared to *PXR* wild-type HL, heterozygous and controls ($p = 0.0001$, $p = 0.0004$ and $p = 0.0001$, respectively). *PXR* homozygous HRS cells had significantly higher PXR expression compared to *PXR* wild-type HRS cells ($p < 0.0001$, 3.27-fold change). Albeit PXR's prominent expression in cytoplasm of HRS cells, homozygous *PXR* HRS cells showed increased PXR expression in nucleus ($p < 0.001$).

PXR is a member of the nuclear receptor superfamily and previous studies have demonstrated a pleiotropic effect of PXR on malignant transformation. Expression analysis showed that cell proliferation, apoptosis and inflammation related genes were deregulated, in homozygous *PXR* HL cases. This study provided clinical evidence to previously reported *Sxr*$^{-/-}$ mice model that develop multifocal lymphomas, had an aberrantly increased NF-κB expression and consistent inflammation. Further functional studies are needed to elucidate the exact mechanisms of action of PXR in HL pathogenesis.

1. Introduction

Hodgkin's lymphoma (HL) is a nodal mature B-cell neoplasm characterised by large multinucleated Reed-Sternberg cells in an inflammatory background. The long-term survival rate in HL exceeds 90% after chemotherapy alone or combined chemotherapy and radiotherapy.

* Corresponding author. Istanbul University, Oncology Institute, Topkapı, Turgut Özal Millet Street No:118, 34093, Fatih, Istanbul, Turkiye.
** Corresponding author. Istanbul University, Aziz Sancar Institute of Experimental Medicine, Topkapı, Gureba Hastanesi Street No:69, 34093, Fatih, Istanbul, Turkiye.
E-mail addresses: mugeay@istanbul.edu.tr (M. Sayitoglu), rejinkebudi@yahoo.com (R. Kebudi).
[1] These authors contributed equally to this work.
[2] These authors contributed equally to this work as Correspondence authors

https://doi.org/10.1016/j.ejmg.2024.104975
Received 17 August 2023; Received in revised form 17 July 2024; Accepted 22 September 2024
Available online 23 September 2024

However, treatment-related cardiovascular disease and increased risk of secondary malignancies are the major problems for HL survivors. Therefore, disease staging, risk stratification and refinement of treatment regimens are the goals of HL therapy in paediatrics (Weniger and Kuppers, 2021; Jardin, 2022). Aberrant activation of the nuclear factor-kappa B (NF-κB) pathway is a hallmark feature of HL, contributing to the survival and proliferation of Hodgkin and Reed-Sternberg (HRS) cells, the malignant cells characteristic of HL. The constitutive activation of NF-κB pathways in HL promotes the expression of genes involved in cell survival, proliferation, and inflammation, thereby promoting tumour growth and immune evasion (Jardin, 2022).

A small percentage of HL cases are associated with cancer predisposition syndromes (i.e. ataxia-telangiectasia (Suarez et al., 2015), Nijmegen breakage syndrome (Wolska-Kusnierz et al., 2015), and primary immunodeficiencies (Schuetz et al., 2007; Khodzhaev et al., 2020; Kebudi et al., 2019)). Genome-wide association studies (GWAS) and family studies, as well as the introduction of next-generation sequencing, are important for the detection of new rare genetic events and the characterisation of genetic susceptibility in HL (Furutani and Shimamura, 2017). Several genes have been reported to be associated with HL predisposition, such as *Nuclear protein, coactivator of histone transcription* (*NPAT), Kelch domain containing 8B (KLHDC8B), Aggrecan (ACAN), Dicer 1, ribonuclease III* (*DICER1), Kinase insert domain receptor (KDR)* and *Protection of telomeres 1 (POT1)* (Szmyd et al., 2021). Although immune dysfunction, exposure to viruses such as Epstein-Barr virus (EBV) or human immunodeficiency virus (HIV), and family history may increase the risk of developing HL, the aetiology and predisposing factors of lymphoma are not well understood. In cases with familial clustering, the identification of genetic predisposition genes in HL may offer therapeutic benefits to index cases and allow genetic counselling and monitoring of family members (Kushekhar et al., 2014; Moutsianas et al., 2011). This study describes a human model of a homozygous variation in a novel candidate gene, *Pregnane X Receptor (PXR)*, found in two siblings with HL in a consanguineous family, for which animal models have been previously described (Casey et al., 2011; Zhou et al., 2006).

2. Material and methods

2.1. Clinical presentations of index case and family members

The family with multiple consanguineous marriages with cases of diagnosed lymphoma was examined in this study (Fig. 1A). Eleven years old index case (IV-10) was diagnosed with inflammatory skin disease at the age of 8 and developed stage IIIBs, nodular sclerosing subtype HL at the age of 10. At diagnosis, she was reported to have bilateral cervical, supraclavicular, axillary lymphadenopathy on physical examination, complaints of weight loss, and drenching night sweats. At diagnosis, on PET CT she was reported to have FDG enhancement in bilateral cervical, supraclavicular, mediastinal, and axillary lymph nodes, and in the spleen. She had received chemotherapy consisting of Adriamycin, Bleomycin, Vinblastine and Dacarbazine (ABVD) at a local hospital. She was reported to have a partial response after three courses, however progressed after six courses. She was referred to our center for further evaluation after disease progression. Her biopsy was re-evaluated, and HL diagnosis was confirmed. CD30 was positive with immunocytochemistry. Patient had a massive, enlarged mediastinum due to conglomerate lymph nodes, nodules in the lung, lymphadenomegalies in the cervical, supraclavicular, and axillary regions. She was treated with chemotherapy consisting of ifosfamide (1.8 g/m^2/d ×5 days) + mesna, carboplatinum (500 mg/m^2/d on day 5), etoposide (100 mg/m^2/d ×5 days) (ICE) and targeted therapy with anti CD30 (brentuximab) and achieved a partial anatomic and complete metabolic response (PET-CT Deauville 1–2 in PET-CT) after six courses (Fig. 1B and C). Stem cell was harvested after three courses and autologous stem cell transplantation (SCT) was performed after six courses. The BEAM regimen (carmustine 300 mg/m2 -7day, etoposide 200 mg/m2 -6,-5,-4,-3.days, cytarabine 2 × 200 g/m2 -6,-5,-4,-3.days, melphalan 140 mg/m2 -2.day) was used as conditioning for SCT. She received 10 monthly courses of brentuximab after SCT. She has been followed in remission and is alive with no evidence of disease for 48 months from initial diagnosis.

Index's 26 years old sister (IV-14) was diagnosed with stage IIA, HL at the age of 24, two months before her sisters' diagnosis. She was pregnant at diagnosis, had a complete response after two courses of ABVD chemotherapy, after that she had a healthy delivery and received additional four courses of ABVD chemotherapy. The parents reported that she had a recurrence in the mediastinal lymph nodes at 44 months after initial diagnosis (38 months after the end of the initial treatment), confirmed by biopsy. She received ICE chemotherapy and targeted treatment with anti-CD30 (brentuximab), achieved complete metabolic remission after three courses and is undergoing autologous stem cell transplant at her local center. Index's 17-years-old sister (IV-12) and her 11-years-old cousin (IV-16) had cervical lymph adenomegalies which had regressed after antibiotherapy. The 21-year-old brother (IV-11) had inflammatory skin findings which were interpreted as chronic inflammatory skin disease. Family members II-7 and III-12 were also diagnosed as inflammatory skin disease. Family members (II-11 and II-13) who were deceased were diagnosed as cirrhosis. The mother developed papillary thyroid cancer 44 months after the HL diagnosis of the index case, she underwent total thyroidectomy and lymph node dissection and had 4/10 lymph nodes positive for tumor and received radioactive iodine treatment at her local city.

This study was approved by Istanbul University Medical Faculty Ethics Board; written and oral informed consents were taken from the family members or legal representatives.

2.2. Genetic analysis

Peripheral blood samples were collected from affected siblings and parents for DNA isolation. Whole exome sequencing (WES) was performed for the index case and Agilent SureSelect Human All ExonV6 (Agilent Technologies, Santa Clara, CA, USA) kit was used for capturing. Illumina's raw data was aligned to hg38 reference genome with Burrows-Wheeler Aligner (BWA) package's (Li and Durbin, 2009) mem algorithm, and Samtools package (Li et al., 2009) was used for Variant Call Format (VCF) file generation. VCF file was annotated with Annovar (Wang et al., 2010). Post-alignment statistics were generated with qualimap (Okonechnikov et al., 2016). Mean sequencing depth was 147x, with 90% of positions in reportable exons covered at >20x. Promoters, untranslated and other non-coding regions were not interrogated (Fig. 1D). Individual and MetaScore values of different available tools (Franklin by Genoox, 2022) (Supplementary Table 1), Combined Annotation Dependent Depletion (CADD) scores (Rentzsch et al., 2019), ClinVar's records (Landrum et al., 2018) and Online Mendelian Inheritance in Man (OMIM) (Hamosh et al., 2005) database was used for variant prioritization. Prioritized variants were classified according to ACMG (American College of Medical Genetics) guidelines (Richards et al., 2015). St Jude's paediatric cancer cohort data was also used for the gene variation states among different cancer types (McLeod et al., 2021). Free energy difference (ΔΔG) was used to assess the impact of the variants on the protein stability by the "Distal Upper Extremity Tool" (DUET) tool (http://biosig.unimelb.edu.au/duet/stability). Gene expression profiling interactive analysis (GEPIA) database was used to evaluate *Pregnane X receptor* (*PXR* or *NR1I2* or *SXR)* expression in different cancer subtypes (Tang et al., 2017).

2.3. Familial segregation, PXR variant and MDR1 haplotype analysis

PXR gene variant validation and segregation analysis were performed by Sanger sequencing. To evaluate the treatment response differences between the siblings a single nucleotide variation (SNVs) of the A*TP binding cassette subfamily B member 1 (ABCB1*) gene (*ABCB1*

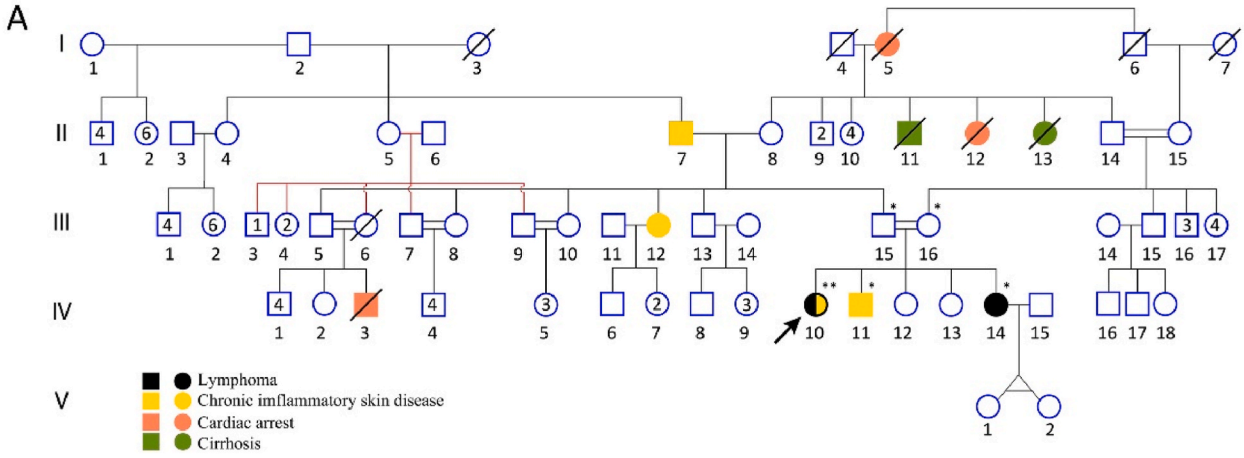

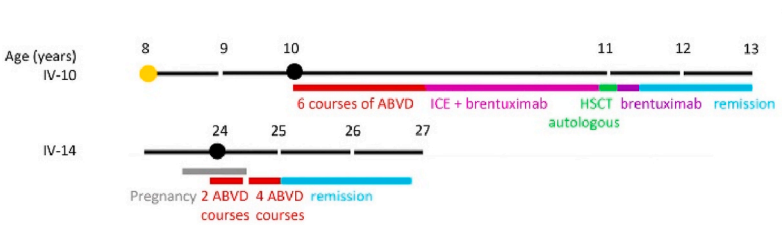

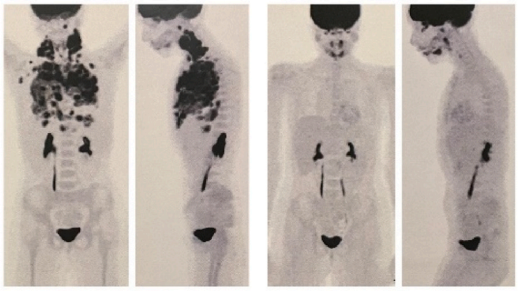

D

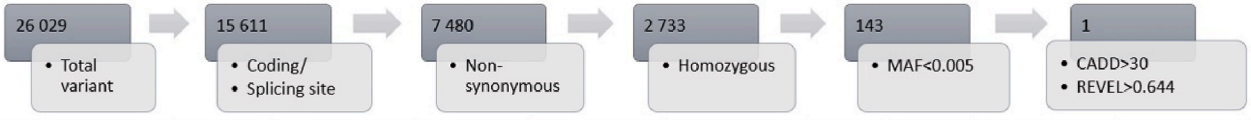

Gene	Refseq	c.DNA	Protein	Exon	dbSNP	GnomAD MAF	CADD	ClinVar	ACMG	REVEL
NR1I2	NM_003889.3	c.811G>A	p.(Asp271Asn)	6	rs144833620	0.00006571	31	VUS	PP2, PM3 (VUS)	Deleterious (0.86)

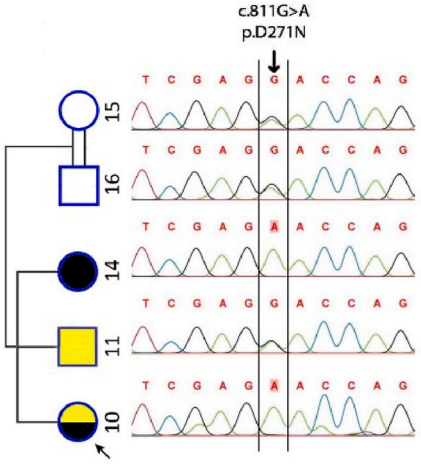

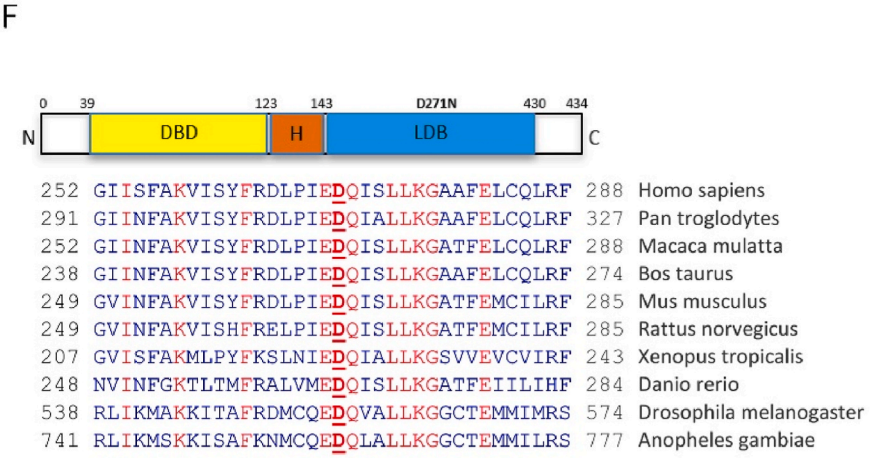

(caption on next page)

Fig. 1. Novel missense NM_003889.3:c.811G > A, p.(Asp271Asn) variant in the *PXR* gene.
A) Pedigree of PXR family including affected members with different clinical phenotypes. Proband (IV-10) is indicated with an arrow. Black symbols represent individuals with Hodgkin lymphoma, yellow - chronic inflammatory skin disease, green - cirrhosis and orange - cardiac arrest. Circles indicate females and squares indicate males; slashes indicate deceased family members. Indicated numbers within squares and circles are number of individuals reported to be healthy. ** denotes samples which underwent both WES and Sanger sequencing and * denotes only Sanger sequencing.
B) Therapy timeline of index case (IV-10) and lymphoma sibling (IV-14). ABVD: Adriamycin, Bleomycin, Vinblastine and Dacarbazine; ICE: of ifosfamide, carboplatin, etoposide; HSCT: hematopoietic stem cell transplantation.
C) PET-CT images of index patient at diagnosis (left) and remission (right)
D) Whole exome sequencing analysis pipeline.
E) Sanger validation and familial segregation of NM_003889.3:c.811G > A, p.(Asp271Asn) variant. V-15 (father), V-16 (mother) and IV-11 (brother) were found heterozygous, and IV-10 (index) and IV-14 (sister) who were diagnosed as Hodgkin Lymphoma were found homozygous.
F) Schematic representation of PXR nuclear hormone receptor domains and conservation of codon 271 aspartic acid (bold and in red) across species and 100% conservation is observed. N –N terminal, C –C terminal, DBD –DNA binding domain, H –hinge, LDB –ligand binding domain. Red amino acids are conserved among represented species and bold underlined red amino acid represents residue with variant. (For interpretation of the references to colour in this figure legend, the reader is referred to the Web version of this article.)

rs1128503, *ABCB1* rs2032582 and *ABCB1* rs1045642) was also evaluated by polymerase chain reaction (PCR) according to the protocol (Thermo Fisher Scientific, Waltham, MA, USA) (Supplementary Table 2). Sanger sequencing analysis were performed using CLC genomics workbench 3.6.5 program (QIAGEN, Aarhus, Denmark).

2.4. Cell culture

HepG2 cells were cultured on the T75 flask in Dulbecco's Modified Eagle Medium high glucose with L-glutamine, foetal bovine serum, and Penicillin-Streptomycin under standard cell culture conditions. Following six days of growth of HepG2, cells were fixed overnight with 0.5% Paraformaldehyde (PFA) and transferred to glass according to cytospin protocol for immunofluorescent staining (Koh, 2013).

2.5. Immunofluorescent staining

PXR expressing HepG2 cells were used as control for immunofluorescent staining. Sections of Formalin -Fixed Paraffin-Embedded (FFPE) samples were taken on glass. Slides were incubated for 1 h at 60 °C and treated with xylene for 30 min. Then slides were incubated within serial alcohol concentrations from 100 to 60% for 5 min respectively. After washing, they were fixed overnight with 0.5% PFA. Samples were incubated with primary antibody (sc-48403, Santa Cruz Biotechnology, Inc., Dallas, TX, USA), secondary antibody (DyLight 488 FITC, Cambridge, UK), and DAPI. Images were acquired by confocal microscope (Leica SP8, Munich, Germany) and analysed using ImageJ (Schneider et al., 2012) program's JACoP plugin (Bolte and Cordelieres, 2006).

2.6. Quantitative real time PCR (qRT-PCR)

Total RNA was isolated from peripheral blood of index case, family members and *PXR*-WT (wild type) patients with HL by using RNeasy Mini Kit (Qiagen, Aarhus, Denmark). Complementary DNA was synthesized using SuperScript™ III First-Strand Synthesis System (Invitrogen by Thermo Fisher Scientific, Carlsbad, CA, USA) according to the instructor's manual. mRNA expression levels for *PXR, Tumour protein p53 (TP53), BCL2 apoptosis regulator (BCL2), MYC proto-oncogene, bHLH transcription factor (MYC), Tumour necrosis factor (TNF), Nuclear factor kappa B subunit 1 (NFKB1), Component of inhibitor of nuclear factor kappa B kinase complex (IKK1), Fas cell surface death receptor (FAS), Lymphoid enhancer binding factor 1 (LEF1), Phosphatase and tensin homolog (PTEN), BCL2 associated X, apoptosis regulator (BAX)* and *Cyclin D1* (*CCND1)* were detected by Quantitative Real-time PCR (qPCR) using specific primers (Supplementary Table 3) and the qPCR SYBR Green Master kit (Roche Diagnostics, Manheim, Germany) on the Light Cycler 480 Instrument (Roche Applied Sciences, Manheim, Germany). *Actin beta* (*ACTB)* expression was used for normalization and samples were run in duplicates. The relative expression levels were calculated by using the ΔΔCt method (Livak and Schmittgen, 2001).

2.7. Statistical analysis

Statistical analyses were done on GraphPad Prism v.9.0 (GraphPad by Dotmatics, Boston, MA, USA) and data presented as mean ± Standard error of the mean (SEM) on box plot with line at mean. Unpaired *t*-test with Welch's correction was used to compare the relative mRNA levels of the samples. Significance level of *p value* was set at <0.05. PXR signal's (green) intensity (green pixel area) was used as comparison parameter in *PXR* expression calculation and *t*-test was used to compare Pearson's Correlation r values, overlap coefficient values and PXR intensity of $PXR^{D271N/D271N}$ and *PXR*-WT HL samples.

3. Results

3.1. Informatic data analysis and familial segregation

WES analysis was performed according to the presented pipeline in Fig. 1D. Pathogenicity was evaluated with prediction tools that listed in Supplementary Table 1, and OMIM and ClinVar reports were used for the clinical interpretation of candidate variants. Homozygous variant of *PXR* was evaluated as the most promising candidate gene in explaining the germline predisposition for lymphomagenesis (NM_003889.3: c.811G > A, p.(Asp271Asn), rs144833620) (Fig. 1D). Segregation analysis with Sanger sequencing verified homozygosity in the HL cases (IV-10 and IV-14) and showed carrier status of the parents (III-13 and III-14) and the brother (IV-11) (Fig. 1E).

PXR c.811G>A, p.(Asp271Asn) was predicted to be pathogenic according to the 11 (MetaLR, MetaSVM, MetaRNN, REVEL, EIGEN, EIGEN PC, FATHMM, FATHMM-MKL, FATHMM-XF, M-CAP, MVP, Mutationtaster, PROVEAN, SIFT4G, SIFT) out of 16 individual prediction tools (Supplementary Table 1) and classified as variant of uncertain significance (VUS) by ACMG criteria (PM2, PM3). This variant is in the ligand binding domain (LBD) of *PXR,* and aspartic acid was seen to be highly conserved across species (Fig. 1F). Furthermore, the *PXR* p.(Asp271Asn), substitution was predicted to impact protein stability (ΔΔG) according to DUET tool (Supplementary Fig. 1). We applied additional filtering for hereditary cancer predisposition gene panel (Supplementary Figs. 2 and 3).

St Jude's paediatric cancer cohort contains no germline *PXR* variant and only three missense variants which are in LBD region was reported in paediatric patients with lymphoid neoplasm. (Supplementary Fig. 4). Patients with Diffuse large B-cell lymphoma (DLBCL) was seen in GEPIA database to have higher expression of *PXR* compared to controls, its expression was stage specific and increased expression was correlated with shorter disease-free survival (Supplementary Fig. 5).

3.2. Clinical presentation of cases with PXR variant

A germline homozygous *PXR* c.811G>A variation was found in two siblings (IV-10 and IV-14) diagnosed with HL. The index case was

referred for further treatment after six courses of chemotherapy. The immunoglobulin (Ig) levels of IgA, IgG, IgM were within normal limits, IgE level was elevated (IgA: 3,72 gr/dl, IgG 18,9 gr/dl, IgM: 2,36 gr/dl, IgE 734 IU/ml). EBV DNA copy number by PCR was not elevated. In the lymphocyte subgroups, the CD4 count was low (132 cell/microliter), CD8 level was high (218 cell/microliter) and CD4/CD8 was 0.6. These values were obtained after six courses of chemotherapy when she was referred to our centre, thus under some immunosuppression and due to progressive disease, she continued immunosuppressive treatment including SCT, thus this and further immunologic workup could not be considered reliable as a baseline immunologic workup to show whether there was an underlying immunodeficiency.

3.3. Increased PXR expression in Hodgkin Reed Sternberg (HRS) cells

We evaluated PXR expression and cell localization in HL samples by immunofluorescence staining. *PXR*$^{D271N/D271N}$ HRS cells had significantly higher PXR expression compared to *PXR*-WT HRS cells ($p < 0.0001$, 3.27-fold change). Albeit PXR's prominent expression in cytoplasm of HRS cells, *PXR*$^{D271N/D271N}$ HRS cells showed increased PXR expression in nucleus ($p < 0.001$) (Fig. 2A and B, Supplementary Fig. 9).

Gene expression level of *PXR* was comparable to protein expression levels for homozygous and WT HL samples. Patients with *PXR*$^{D271N/D271N}$ showed significantly high expression compared to *PXR* WT HL, *PXR*$^{WT/D271N}$ and healthy control samples (HC) ($p=0.0001$, $p=0.0004$ and $p=0.0001$, respectively) (Fig. 2C).

3.4. Deregulated inflammation and apoptosis pathways related gene expressions in HL patient with PXR variant

To be able to show the NF-κB signaling activation, we examined the *NFKB1, IKK1* and *TNF* expression profile in HL and HC. HL samples with *PXR*$^{D271N/D271N}$ variant showed relatively higher *NFKB1* expression compared to *PXR*-WT HL (p=0.0551), *PXR*$^{WT/D271N}$ carriers (p=0.0707) and HC groups (p=0.0550). *PXR*$^{D271N/D271N}$ HL samples had relatively increased *IKK1* expression level compared to *PXR*-WT HL (p=0.2016), *PXR*$^{WT/D271N}$ carriers (p=0.2117) and HC groups (p=0.2024). *PXR*$^{D271N/D271N}$ HL samples with variant showed relatively increased *TNF* expression level compared to *PXR*-WT HL (p=0.0899), *PXR*$^{WT/D271N}$ carriers (p=0.1478) and HC (p=0.0997) (Fig. 2C).

Here we examined the apoptotic genes' expression of *TP53, BCL2, FAS, BAX* in HL and controls. We found significant reductions for *TP53, BCL2, FAS* expressions in the *PXR*$^{D271N/D271N}$ HL samples compared to *PXR*$^{WT/D271N}$ carriers and HC for *TP53* $p=0.0021$ and $p=0.0001$, for *BCL2* $p= 0.0142$ and $p=0.0002$, for *FAS* $p=0.0190$ and $p=0.0003$ respectively. Expression levels of *TP53, BCL2, FAS* in *PXR*$^{D271N/D271N}$ samples were similar to *PXR*-WT HL (p=0.0741, p=0.0801 and p=0.084, respectively) (Supplementary Fig. 6). *BAX* gene expression levels were not significant between the *PXR*$^{D271N/D271N}$ and *PXR*$^{WT/D271N}$ individuals (p=0.5912) and *PXR*$^{D271N/D271N}$ vs. HC (p=0.2746), whereas *PXR*-WT HL samples showed decreased *BAX* expression compared to *PXR*$^{D271N/D271N}$ samples.

Lower *MYC* expression was detected in samples with *PXR*$^{D271N/D271N}$ compared to *PXR*-WT HL, *PXR*$^{WT/D271N}$ and HC ($p=0.0058$, $p=0.0051$ and $p=0.0001$, respectively). Homozygous HL samples had also significantly decreased *LEF1* expression compared to the controls (*PXR*$^{D271N/D271N}$ *vs* *PXR*$^{WT/D271N}$ $p=0.0397$, *PXR*$^{D271N/D271N}$ samples vs HC $p=0.0017$) but increased compared to *PXR*-WT HL samples ($p < 0.0001$) (Supplementary Figs. 6D and 6E).

Samples with *PXR*$^{D271N/D271N}$ alteration did not show any differential expression for *CCND1* (*PXR*$^{D271N/D271N}$ samples compared to *PXR*-WT HL ($p=0.4641$), *PXR*$^{WT/D271N}$ samples ($p=0.0956$) and HC ($p=0.2988$) (Supplementary Fig. 7B). *PXR*-WT HL samples showed significantly reduced *PTEN1* expression compared to *PXR*$^{D271N/D271N}$ samples ($p=0.0001$) (Supplementary Fig. 7C).

When protein interaction network was evaluated (Supplementary Fig. 10), PXR was seen to be directly interacting with NF-kB related proteins through TP53 and TNF.

3.5. ABCB1 haplotypes in siblings

To evaluate the different treatment responses between the sisters (IV-10 and IV-14) with HL, we checked two important *PXR* target genes; multidrug resistance 1 (*MDR1*) and cytochrome P450 3A4 (*CYP3A4*) for the possible metabolic polymorphisms. Index case (IV-10) did not show any functional polymorphism in the *CYP3A4* gene. But a specific *MDR1* haplotype was found homozygous for all three rs1128503, rs2032582 and rs1045642 variants in index case (IV-10), the sister (VI-14) who had good response to chemotherapy and the brother (IV-11) were heterozygous for the same polymorphic regions (Supplementary Fig. 8).

4. Discussion

PXR is a member of the nuclear receptor superfamily and germline variations of *PXR* have been associated with treatment response and resistance in cancers. Dysregulated PXR expression has been reported in different cancer types and previous studies have demonstrated a pleiotropic effect of PXR on malignant transformation. PXR activation has been shown to affect proliferation, apoptosis, cell cycle and drug metabolism through target gene expression (Casey et al., 2011; Pondugula et al., 2016; Xing et al., 2020; Skandalaki et al., 2021)

The cellular function of PXR, is largely achieved through ligand-dependent binding to regulatory gene sequences. *PXR* has a highly conserved DNA-binding domain (DBD) and a ligand-binding domain (LBD), which includes the ligand-dependent activation function 2 (AF2) region and the ligand-binding pocket. Upon ligand binding in AF2, conformational changes occur that subsequently affect the transcription of target genes (Xing et al., 2020). Herein, we identified a germline homozygous *PXR* gene variation p.(Asp271Asn) in two sisters with HL which is located in LBD of *PXR* and predicted to affect protein stability (ΔΔG). There is evidence that variations in this region alter target gene expression through conformational changes.

Activation of the NF-κB pathway is a well characterized and known mechanism in sporadic HL, and germline gene variations that cause NF-κB pathway activation have also been reported in HL. While there is no direct evidence that *PXR* variations confer germline susceptibility to HL, the development of age-related B-cell lymphoma has been observed in an *Sxr−/−* mouse model with abnormally increased expression of NF-κB and its target genes (Casey et al., 2011). Zhou et al. confirmed that NF-κB target genes are upregulated in mice lacking *Sxr* and that NF-κB activation reciprocally inhibits *Sxr*, whereas NF-κB inhibition enhances Sxr activity (Zhou et al., 2006). In this respect, NF-κB related genes' expressions, which were shown in these animal models to be deregulated were evaluated in *PXR* mutated family members (cell proliferation (*Chuk, Nfkb1*), apoptosis (*p53, Bcl-2, Fas*) and inflammation (*TNFα*) related genes). In parallel with the findings in animal models, these genes were found to be deregulated in homozygous *PXR* HL cases presented in our study. To evaluate the effect of the *PXR* variation on gene/protein levels and cellular localization, we examined *PXR*$^{WT/D271N}$ and WT individuals as well as HL patient samples without *PXR* variant. *PXR* expression levels were significantly increased in homozygous individuals in all comparison groups. Furthermore, both total and nuclear PXR levels were found to be elevated in HRS cells with *PXR* variant. PXR is involved in the modulation of different biological processes, including inflammation, apoptosis, cell cycle arrest, lipid and drug metabolism (Pondugula et al., 2016). Our study expanded the data on NF-κB pathway activation in HRS cells that indicated a new *PXR* mediated route for aberrant lymphomagenesis. *PXR* variant might impair the regulation of NF-κB affecting the apoptosis related gene expression and increase cell proliferation in HRS cells (Supplementary Fig. 10). Since both *PXR* and NF-κB related genes are found to be upregulated, a possible explanation might be that the homozygous variant in LBD

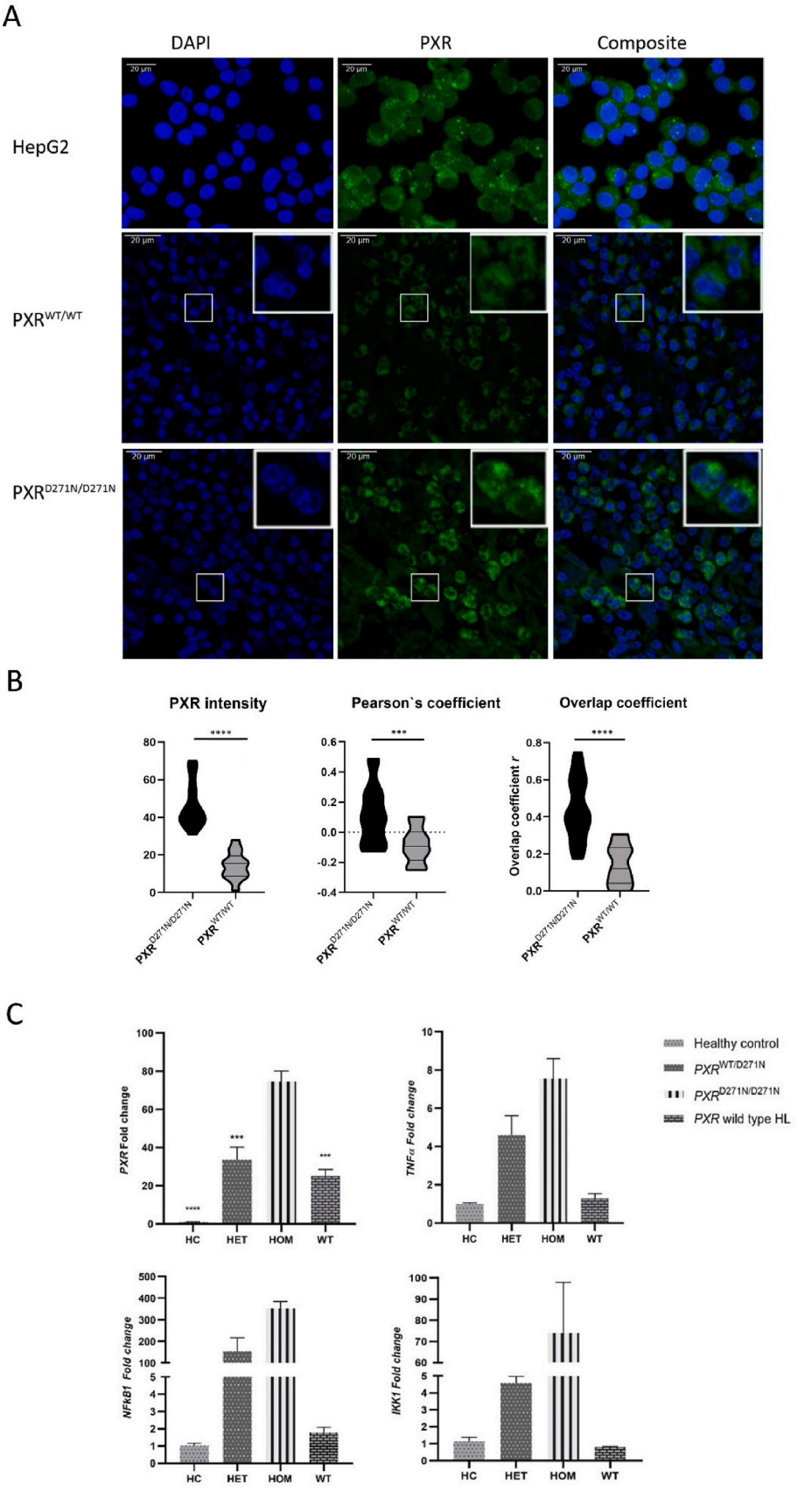

(caption on next page)

Fig. 2. PXR protein expression and *PXR, TNFα, IKK1* and *NFKB1* mRNA expressions at HL and control cells.
A. Multinuclear HRS cells express PXR in HL tissues. Immunofluorescence staining utilizing a primary antibody against PXR (green) and DAPI (blue) staining for nucleus. HepG2 cell line is used as a positive control for PXR expression. Depicted white squares are zoomed to representative images of the PXR expression at HRS cells. Confocal images showed prominent cytoplasmic expression of PXR at $PXR^{D271N/D271N}$ (IV-14) HRS cells compared to *PXR* wild type HRS cells. All images were acquired at *40 × magnification,* Scale bars, 20 μm.
B. Protein quantification results were presented as the ratio of cells showing nuclear PXR expression to cells showing cytoplasmic expression in comparison to *PXR* wild type and $PXR^{D271N/D271N}$. Significantly increased PXR expression was detected in $PXR^{D271N/D271N}$ cells. Data are represented as mean ± s.e.m. Unpaired *t*-test was used to compare mean between groups. In each group, HRS cells were selected for quantification ($PXR^{D271N/D271N}$ HRS cells n = 16; *PXR* wild type HRS cells n = 13). PXR intensity graph shows PXR's (green) value in pixels (area); Pearson's coefficient graph depicts correlation r values of PXR and DAPI detected pixels and overlap coefficient graph overlap coefficient r values between PXR and DAPI staining pixels in HRS cells. Dashed line in Pearson's coefficient graph corresponds to the 0 of r value.
C. Gene expression levels of *PXR, TNFα, IKK1* and *NFKB1* in $PXR^{D271N/D271N}$ (IV-10 (index) and IV-14 (sister)) and *PXR* wild type patients with HL, healthy $PXR^{WT/D271N}$ carriers (IV-11 (brother), III-15 (father), III-16 (mother)) and *PXR* wild type healthy controls. $PXR^{D271N/D271N}$ HL samples had relatively increased *PXR, TNF, IKK1* and *NFKB1* expressions compare to other groups. *ACTB* gene was used for normalization. Mean ± s.e.m. of duplicate measurements are depicted. *p value* significance: **** - ≤0.0001 and *** - ≤0.001. Indicated significance levels above bars are *p values* of comparison with $PXR^{D271N/D271N}$ group. Y axis was represented as fold change compared to healthy control group. HOM: $PXR^{D271N/D271N}$ HL; HET: healthy $PXR^{WT/D271N}$ heterozygous family members; WT: *PXR* wild type HL samples; HC: *PXR* wild type healthy controls. (For interpretation of the references to colour in this figure legend, the reader is referred to the Web version of this article.)

disrupts the PXR response to ligands and its downstream effects, including NF-κB suppression which may have led to lymphomagenesis. However, further functional studies are required to verify our findings.

PXR expression down regulates p53 activity independently of its transactivation activity and inhibits its downstream targets involved in cell cycle arrest and apoptosis in human immune cells (Robbins et al., 2016). It has been noted that PXR physically interacts (in a ligand dependent manner) with p53, promotes malignant transformation by reduced apoptosis, but their direct mutual inhibition is not clear. In the current study, proapoptotic genes, *p53* and *BCL*-2 that were found downregulated in HL with *PXR* variant suggesting the downstream effect of PXR in malignant transformation through reduced apoptosis.

Additionally, heterozygous *PXR* variant cause inflammation by upregulating *TNFα* expression which is a possible mechanism of chronic inflammatory skin findings in family members of this study. *PXR* is expressed in cutaneous tissue and plays role in cutaneous homeostasis (Schmuth et al., 2014). The mouse model created by Elentner et al. showed that constitutive activation of *PXR* in the epidermis results in impaired epidermal barrier and triggers atopy. *PXR* expression was also found increased in the skin of patients with atopic dermatitis (Elentner

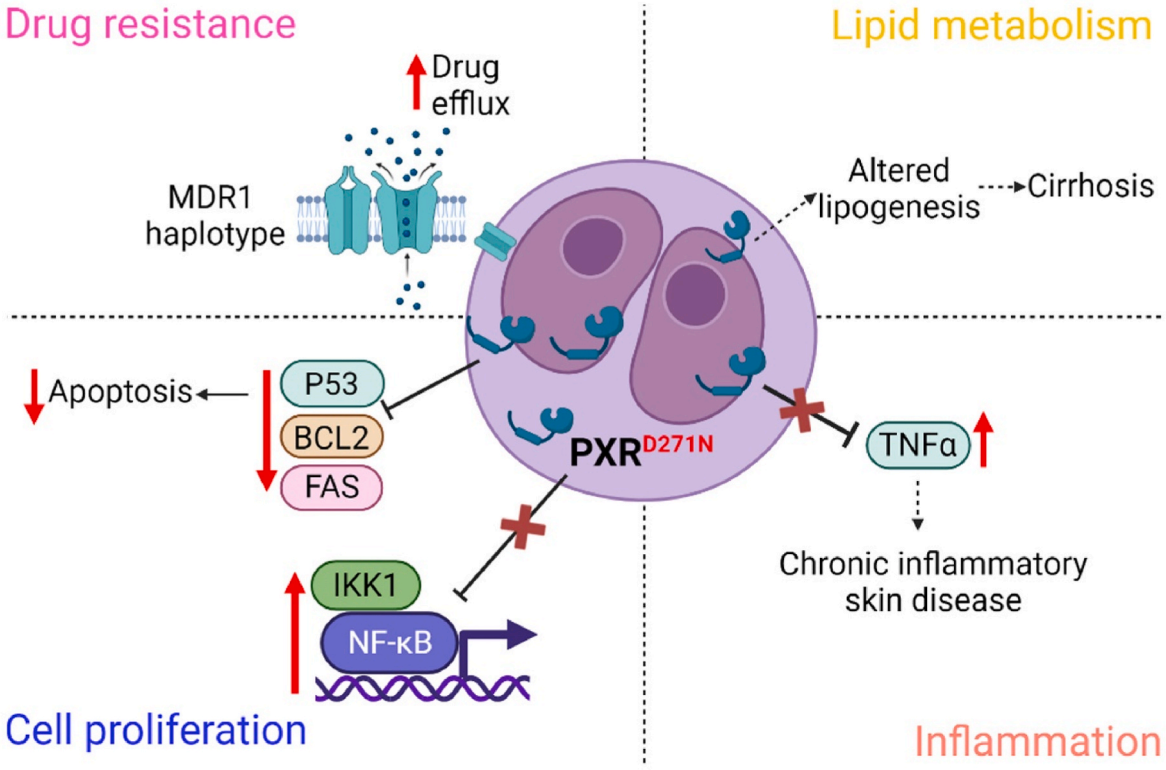

Fig. 3. Possible impact for PXR with variant in Hodgkin Reed Sternberg cells.
PXR is a ligand-activated transcription factor and involved in the modulation of different biological processes, including inflammation, apoptosis, cell cycle arrest, lipid and drug metabolism. PXR variant can cause impaired regulation of NF-κB and leads to decreased apoptosis related gene expression profile and increased cell proliferation in Hodgkin Reed Sternberg cells. PXR with variant can also cause inflammation by upregulating TNFα expression which is a possible mechanism of chronic inflammatory skin findings in family members. PXR is highly expressed by hepatocytes that regulate glucose and lipid metabolism. Aberrant expression of PXR can contribute to cirrhosis findings in deceased individuals. MDR haplotypes were determined to pump out anti-cancer agents from cells that cause reduced drug effectiveness. Drug resistance related MDR1 haplotype's association with poor therapy response seen in index HL case. Image was generated at https://biorender.com.

et al., 2018). *PXR* is highly expressed by hepatocytes that regulate glucose and lipid metabolism so aberrant expression of PXR might contribute to cirrhosis findings in deceased individuals in our extended family (Fig. 3).

Our study provided clinical evidence for the previously reported Sxr−/− mouse model, which develops multifocal lymphomas, has aberrantly increased *Nfkb1* expression and persistent inflammation. The germline homozygous PXR c.811G > A variant found in two HL siblings may lead to upregulated nuclear PXR levels in HRS cells. Analysis of the primary patient samples also revealed NF-κB activation and inflammation, which may trigger the development of HL. Germline PXR variation is a rare event in cancer, and the family presented here with different phenotypic presentations, including HL, inflammatory skin disease and cirrhosis, supports the impaired functions of PXR for the first time. Further functional studies are needed to understand the role of PXR in lymphomagenesis.

Funding sources

This study was funded by Scientific Research Projects Coordination Unit of Istanbul University, Project number: TDK-2022-38816, TDK-2020-37127, TSA-2023-39470 and General Directorate of Development Agencies, Istanbul Development Agency Project number: TR10/22/TNH/0001.

Ethical approval

This study was approved by Istanbul University Medical Faculty Ethics Board; written and oral informed consents were taken from the family members or legal representatives.

CRediT authorship contribution statement

Khusan Khodzhaev: Writing – review & editing, Writing – original draft, Investigation. **Tugce Sudutan:** Writing – review & editing, Writing – original draft, Investigation. **Yucel Erbilgin:** Writing – review & editing, Writing – original draft, Investigation. **Merve Saritas:** Writing – review & editing, Writing – original draft, Investigation. **Gulcin Yegen:** Writing – review & editing, Writing – original draft, Investigation. **Ceyhun Bozkurt:** Writing – review & editing, Writing – original draft, Investigation. **Muge Sayitoglu:** Writing – review & editing, Writing – original draft, Supervision, Investigation. **Rejin Kebudi:** Writing – review & editing, Writing – original draft, Supervision, Investigation.

Declaration of competing interest

The authors declare that they have no known competing financial interests or personal relationships that could have appeared to influence the work reported in this paper.

Data availability

Data will be made available on request.

Acknowledgments

We thank the family for participating in the study, and Julide Hocaoglu for assistance in cutting FFPE sections.

Appendix A. Supplementary data

Supplementary data to this article can be found online at https://doi.org/10.1016/j.ejmg.2024.104975.

References

Bolte, S., Cordelieres, F.P., 2006. A guided tour into subcellular colocalization analysis in light microscopy. J Microsc 224 (Pt 3), 213–232. https://doi.org/10.1111/j.1365-2818.2006.01706.x.

Casey, S.C., Nelson, E.L., Turco, G.M., Janes, M.R., Fruman, D.A., Blumberg, B., 2011. B-1 cell lymphoma in mice lacking the steroid and xenobiotic receptor, SXR. Mol. Endocrinol. 25 (6), 933–943. https://doi.org/10.1210/me.2010-0486.

Elentner, A., Schmuth, M., Yannoutsos, N., et al., 2018. Epidermal overexpression of xenobiotic receptor PXR impairs the epidermal barrier and triggers Th2 immune response. J. Invest. Dermatol. 138 (1), 109–120. https://doi.org/10.1016/j.jid.2017.07.846.

Franklin by Genoox. https://franklin.genoox.com, 2022.

Furutani, E., Shimamura, A., 2017. Germline genetic predisposition to hematologic malignancy. J. Clin. Oncol. 35 (9), 1018–1028. https://doi.org/10.1200/JCO.2016.70.8644.

Hamosh, A., Scott, A.F., Amberger, J.S., Bocchini, C.A., McKusick, V.A., 2005. Online Mendelian Inheritance in Man (OMIM), a knowledgebase of human genes and genetic disorders. Nucleic Acids Res. 33 (Database issue), D514–D517. https://doi.org/10.1093/nar/gki033.

Jardin, F., 2022. NFkB pathway and hodgkin lymphoma. Biomedicines 10 (9). https://doi.org/10.3390/biomedicines10092153.

Kebudi, R., Kiykim, A., Sahin, M.K., 2019. Primary immunodeficiency and cancer in children; A review of the literature. Curr. Pediatr. Rev. 15 (4), 245–250. https://doi.org/10.2174/1573396315666190917154058.

Khodzhaev, K., Bay, S.B., Kebudi, R., et al., 2020. Lymphoma predisposing gene in an extended family: CD70 signaling defect. J. Clin. Immunol. 40 (6), 883–892. https://doi.org/10.1007/s10875-020-00816-4.

Koh, C.M., 2013. Preparation of cells for microscopy using cytospin. Methods Enzymol. 533, 235–240. https://doi.org/10.1016/B978-0-12-420067-8.00016-7.

Kushekhar, K., van den Berg, A., Nolte, I., Hepkema, B., Visser, L., Diepstra, A., 2014. Genetic associations in classical hodgkin lymphoma: a systematic review and insights into susceptibility mechanisms. Cancer Epidemiol. Biomarkers Prev. 23 (12), 2737–2747. https://doi.org/10.1158/1055-9965.EPI-14-0683.

Landrum, M.J., Lee, J.M., Benson, M., et al., 2018. ClinVar: improving access to variant interpretations and supporting evidence. Nucleic Acids Res. 46 (D1), D1062–D1067. https://doi.org/10.1093/nar/gkx1153.

Li, H., Durbin, R., 2009. Fast and accurate short read alignment with Burrows-Wheeler transform. Bioinformatics 25 (14), 1754–1760. https://doi.org/10.1093/bioinformatics/btp324.

Li, H., Handsaker, B., Wysoker, A., et al., 2009. The sequence alignment/map format and SAMtools. Bioinformatics 25 (16), 2078–2079. https://doi.org/10.1093/bioinformatics/btp352.

Livak, K.J., Schmittgen, T.D., 2001. Analysis of relative gene expression data using real-time quantitative PCR and the 2(-Delta Delta C(T)) Method. Methods 25 (4), 402–408. https://doi.org/10.1006/meth.2001.1262.

McLeod, C., Gout, A.M., Zhou, X., et al., 2021. St. Jude cloud: a pediatric cancer genomic data-sharing ecosystem. Cancer Discov. 11 (5), 1082–1099. https://doi.org/10.1158/2159-8290.CD-20-1230.

Moutsianas, L., Enciso-Mora, V., Ma, Y.P., et al., 2011. Multiple Hodgkin lymphoma-associated loci within the HLA region at chromosome 6p21.3. Blood 118 (3), 670–674. https://doi.org/10.1182/blood-2011-03-339630.

Okonechnikov, K., Conesa, A., Garcia-Alcalde, F., 2016. Qualimap 2: advanced multi-sample quality control for high-throughput sequencing data. Bioinformatics 32 (2), 292–294. https://doi.org/10.1093/bioinformatics/btv566.

Pondugula, S.R., Pavek, P., Mani, S., 2016. Pregnane X receptor and cancer: context-specificity is key. Nucl Receptor Res, 3doi. https://doi.org/10.11131/2016/101198.

Rentzsch, P., Witten, D., Cooper, G.M., Shendure, J., Kircher, M., 2019. CADD: predicting the deleteriousness of variants throughout the human genome. Nucleic Acids Res. 47 (D1), D886–D894. https://doi.org/10.1093/nar/gky1016.

Richards, S., Aziz, N., Bale, S., et al., 2015. Standards and guidelines for the interpretation of sequence variants: a joint consensus recommendation of the American College of medical genetics and genomics and the association for molecular pathology. Genet. Med. 17 (5), 405–424. https://doi.org/10.1038/gim.2015.30.

Robbins, D., Cherian, M., Wu, J., Chen, T., 2016. Human pregnane X receptor compromises the function of p53 and promotes malignant transformation. Cell Death Discov 2, 16023. https://doi.org/10.1038/cddiscovery.2016.23.

Schmuth, M., Moosbrugger-Martinz, V., Blunder, S., Dubrac, S., 2014. Role of PPAR, LXR, and PXR in epidermal homeostasis and inflammation. Biochim. Biophys. Acta 1841 (3), 463–473. https://doi.org/10.1016/j.bbalip.2013.11.012.

Schneider, C.A., Rasband, W.S., Eliceiri, K.W., 2012. NIH Image to ImageJ: 25 years of image analysis. Nat. Methods 9 (7), 671–675. https://doi.org/10.1038/nmeth.2089.

Schuetz, C., Barbi, G., Barth, T.F., et al., 2007. ICF syndrome: high variability of the chromosomal phenotype and association with classical Hodgkin lymphoma. Am. J. Med. Genet. 143A (17), 2052–2057. https://doi.org/10.1002/ajmg.a.31885.

Skandalaki, A., Sarantis, P., Theocharis, S., 2021. Pregnane X receptor (PXR) polymorphisms and cancer treatment. Biomolecules 11 (8). https://doi.org/10.3390/biom11081142.

Suarez, F., Mahlaoui, N., Canioni, D., et al., 2015. Incidence, presentation, and prognosis of malignancies in ataxia-telangiectasia: a report from the French national registry of primary immune deficiencies. J. Clin. Oncol. 33 (2), 202–208. https://doi.org/10.1200/JCO.2014.56.5101.

Szmyd, B., Mlynarski, W., Pastorczak, A., 2021. Genetic predisposition to lymphomas: overview of rare syndromes and inherited familial variants. Mutat Res Rev Mutat Res. 788, 108386. https://doi.org/10.1016/j.mrrev.2021.108386.

Tang, Z., Li, C., Kang, B., Gao, G., Li, C., Zhang, Z., 2017. GEPIA: a web server for cancer and normal gene expression profiling and interactive analyses. Nucleic Acids Res. 45 (W1), W98–W102. https://doi.org/10.1093/nar/gkx247.

Wang, K., Li, M., Hakonarson, H., 2010. ANNOVAR: functional annotation of genetic variants from high-throughput sequencing data. Nucleic Acids Res. 38 (16), e164. https://doi.org/10.1093/nar/gkq603.

Weniger, M.A., Kuppers, R., 2021. Molecular biology of Hodgkin lymphoma. Leukemia 35 (4), 968–981. https://doi.org/10.1038/s41375-021-01204-6.

Wolska-Kusnierz, B., Gregorek, H., Chrzanowska, K., et al., 2015. Nijmegen breakage syndrome: clinical and immunological features, long-term outcome and treatment options - a retrospective analysis. J. Clin. Immunol. 35 (6), 538–549. https://doi.org/10.1007/s10875-015-0186-9.

Xing, Y., Yan, J., Niu, Y., 2020. PXR: a center of transcriptional regulation in cancer. Acta Pharm. Sin. B 10 (2), 197–206. https://doi.org/10.1016/j.apsb.2019.06.012.

Zhou, C., Tabb, M.M., Nelson, E.L., et al., 2006. Mutual repression between steroid and xenobiotic receptor and NF-kappaB signaling pathways links xenobiotic metabolism and inflammation. J. Clin. Invest. 116 (8), 2280–2289. https://doi.org/10.1172/JCI26283.